IEEE Access
Multidisciplinary ⋮ Rapid Review ⋮ Open Access Journal

Received 10 June 2024, accepted 3 July 2024, date of publication 8 July 2024, date of current version 16 July 2024.

Digital Object Identifier 10.1109/ACCESS.2024.3424466

RESEARCH ARTICLE

Self-Supervised Seismic Random Noise Suppression With Higher-Quality Training Data Based on Similarity Differences

JIAN GAO[1,2], ZHENCHUN LI[1,2], MIN ZHANG[1,2], WANYUE GAO[3], AND YIXUAN GAO[4]

[1]State Key Laboratory of Deep Oil and Gas, China University of Petroleum (East China), Qingdao 266580, China
[2]School of Earth Science and Technology, China University of Petroleum (East China), Qingdao 266500, China
[3]Business School, Shandong Normal University, Jinan 250358, China
[4]School of Biological Science, Qufu Normal University, Qufu 273165, China

Corresponding authors: Zhenchun Li (leonli@upc.edu.cn) and Jian Gao (1946595208@qq.com)

This work was supported in part by the Major Science and Technology Cooperation Projects of China National Petroleum Corporation under Grant ZD2019-183-003, and in part by the National Natural Science Foundation of China under Grant 42074133.

ABSTRACT Suppressing random noise and improving the signal-to-noise ratio of seismic data holds immense significance for subsequent high-precision processing. As one of the most widely used denoising methods, self-learning-based algorithms typically partition the large zone into several smaller zones for individual training and processing, thereby achieving lower training costs. However, as the volume of seismic data that needs to be processed continues to increase, the cost advantage of this method becomes less apparent. This is because a larger data volume necessitates more independent training, ultimately increasing the overall training cost. Therefore, we propose a denoising method based on self-supervised learning to overcome the aforementioned problem. This method can directly acquire higher-quality training data from large zones by leveraging similarity differences, decreasing the need to divide the large zone into smaller parts for individual processing. As a result, it can effectively reduce the times for individual processing, leading to a decrease in the overall training cost. Compared to traditional denoising methods and self-supervised learning methods, the experimental results on both synthetic and field data demonstrate that the proposed denoising method exhibits superior performance in random noise attenuation and reduction in training costs.

INDEX TERMS Seismic data, random noise, deep learning, self-supervised learning.

I. INTRODUCTION

With the growing emphasis on deep and ultra-deep seismic exploration, the need for high-precision geological exploration is becoming increasingly evident. High-precision seismic exploration necessitates a high signal-to-noise ratio (SNR) of seismic data, which significantly impacts subsequent seismic data inversion and geological interpretation [1]. However, during the process of seismic data acquisition, it inevitably becomes contaminated by noise, which can be categorized into coherent noise and random noise. Random noise, typically caused by various disturbances in the acquisition environment, does not possess a fixed frequency or apparent velocity. Consequently, this random noise has the potential to significantly diminish the SNR of seismic data and introduce substantial disruptions to subsequent seismic data processing. Hence, the suppression of random noise in seismic data has garnered considerable attention among researchers.

To suppress random noise in seismic data, numerous methods have been proposed. These include prediction filtering methods such as FX deconvolution (FX), transform domain filtering methods like wavelet transform (WT), modal decomposition methods exemplified by variational

The associate editor coordinating the review of this manuscript and approving it for publication was Geng-Ming Jiang.

mode decomposition (VMD), rank-reduction methods like multi-channel singular value analysis (MSSA), and deep learning methods including convolutional neural networks. The premise of prediction filtering methods [2], [3], [4], [5] is that effective seismic signals can be anticipated in the frequency-space or time-space domain, while random noise remains unpredictable. Leveraging this disparity in predictive characteristics allows for the design of suitable filter operators to mitigate random noise in the frequency domain. Clean data can then be procured through a subsequent inverse transformation. Approaches for filtering in the transform domain [6], [7], [8], [9] can convert the seismic data into a designated transform domain, and subsequently apply specific thresholds to perform denoising. These thresholds are formulated based on the distinguishable disparity between effective signals and random noise within the transform coefficients. Despite their proficiency in mitigating random noise, these methods rooted in transform-domain often fail to entirely eradicate noise. In other words, they invariably blend a portion of the noise with valid data, resulting in residual noise. Modal decomposition methods [10], [11], [12], [13] strive to enhance signal reconstruction and attenuate random noise by breaking down seismic data into several signal components and superimposing the primary components that represent the clean data. However, this decomposition process could inadvertently cause the clean data and noise to intermix. Consequently, this can lead to multiple signal components with indeterminable mix ratios, resulting in a potential loss of effective signal and residual noise in the denoised output. Rank-reduction methodologies [14], [15], [16], [17] posit that the optimal clean data can be formulated as a low-rank matrix. The objective is to attenuate the rank augmentation induced by the random noise present in the seismic signal matrix, thereby facilitating noise suppression. Machine learning methodologies, with their innovative and efficient approach to data processing tasks, have gained substantial traction. Among these, techniques based on deep learning, particularly those employing Convolutional Neural Networks (CNNs), have witnessed significant advancement. This progress has not been lost in the field of seismic denoising, where numerous methods [18], [19], [20], [21], [22], [23], [24], [25] have been proposed that leverage deep learning to effectively suppress random noise. These methodologies have proven pivotal in enhancing the signal-to-noise ratio (SNR) of seismic data and attenuating random noise, thus providing a conducive environment for subsequent inversion and geological interpretation.

In recent years, researchers have tended to use self-supervised methods [18], [26] rather than supervised methods for random noise attenuation, due to the high training cost (high calculation cost and high training data building cost) of supervised learning. These self-supervised methods can be directly applied to test data without the need for additional training data construction, and have less calculation cost. These methods leverage the disparity in correlation between valid data and random noise in the inputs and labels to suppress random noise. Their objective is to find a way to cause correlation discrepancy between seismic signals and random noise, which influences the network's learning process. A higher correlation between inputs and labels results in a higher learning rate of the network. Consequently, the network can construct a model with a denoising effect by prioritizing finishing the learning to valid data.

TABLE 1. Network training comparisons for synthetic example.

Information	MRN-NEW	MRN-OLD
Preparation time (s)	124.81	4.62
Training time (s)	140	168
Pixel number for training	1,140,000	38,400
Computational cost per pixel (s)	**0.000232**	**0.004495**

However, as the amount of test data increases, especially for self-supervised methods that reorganize data to achieve difference, it is not practical to train the network using all of the test data. This is because it can make it harder for the network to learn from valid data and reduce the difference between valid data and noise. This could increase the risk of failure in building the denoising model. If the test data is divided into smaller parts for separate training and processing, the overall cost may no longer be advantageous despite the low cost of individual processing, due to the increased times of separate processes. In addition, complex geological structures typically represent a small portion of the overall data. When using these self-supervised methods, this proportion is also reflected in the training data. As a result, processing for these complex structures is less effective compared to processing for other common and relatively simple structures.

Therefore, we proposed an improved self-supervised denoising method based on data reorganization. This method first selects high-quality zones from all the test data for training. Then, it constructs training data from the selected zones. Finally, it performs general self-supervised training to build the denoising model. Compared to conventional self-supervised denoising methods, this method utilizes high-quality zone selection to decrease the times for individual processing, thereby reducing the overall cost. Additionally, high-quality zone selection can easily acquire the data containing complex structures, thereby increasing the proportion of data representing these structures. This means this method can perform better in processing complex structures.

The rest of this paper is organized as follows. Section II mainly presents the proposed denoising strategy and selection strategy. Section III introduces the M-ResUNet [26]. In Section IV, experiments are conducted on synthetic and field data to demonstrate the effectiveness of the proposed method in attenuating random noise and reconstructing signals. Finally, Section V concludes this paper.

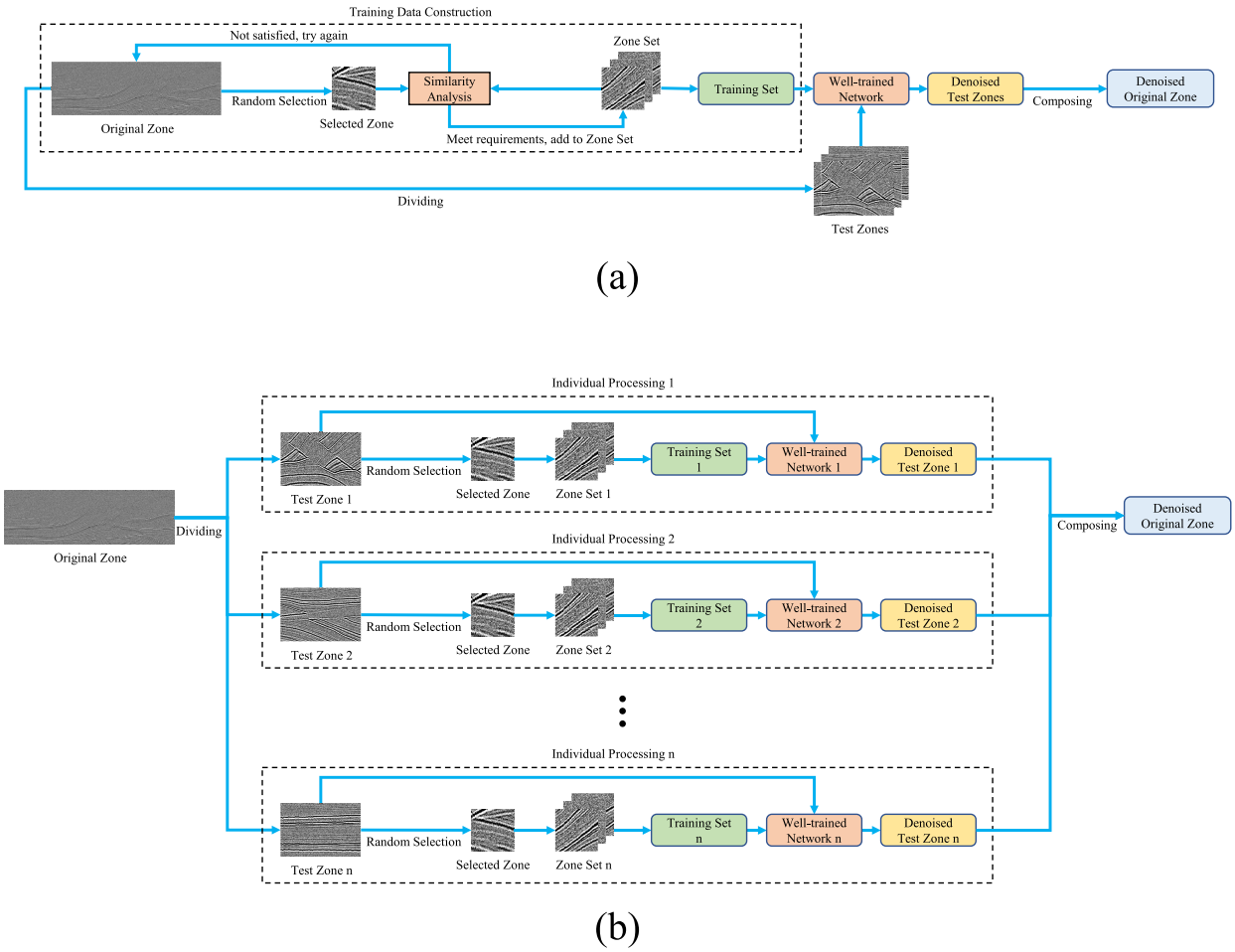

FIGURE 1. Processing flows of the self-supervised methods for the original zone. (a) The proposed method (MRN-NEW). (b) Conventional self-supervised method for comparison (MRN-OLD).

TABLE 2. SNR and RMSE of the synthetic results [SNR (dB)/RMSE].

Noisy data	MRN-NEW	MRN-OLD	MSSA	FX	WT	VMD
2.478/0.082	**6.894/0.049**	7.292/0.047	4.954/0.062	4.690/0.065	2.560/0.083	1.287/0.094
-0.596/0.115	**6.158/0.053**	6.190/0.053	2.331/0.082	3.969/0.068	2.168/0.084	0.709/0.099
-3.309/0.162	**5.486/0.059**	5.501/0.059	-0.144/0.113	2.762/0.081	2.081/0.087	-0.335/0.115
-5.998/0.218	**4.305/0.067**	2.061/0.086	-2.839/0.152	1.130/0.096	1.447/0.093	-1.913/0.136
-8.794/0.312	**2.709/0.083**	-0.168/0.115	-5.476/0.0.213	-0.250/0.117	1.057/0.100	-3.380/0.177

TABLE 3. Network training comparisons for field example.

Information	MRN-NEW	MRN-OLD
Preparation time (s)	126.52	4.43
Training time (s)	152	147
Pixel number for training	2,000,000	38,400
Computational cost per pixel (s)	**0.000139**	**0.003944**

II. METHODS

A. DENOISING STRATEGY

As we know, the seismic data ($Y_{m,t}$) can be expressed as follows:

$$Y_{m,t} = X_{m,t} + noise_{m,t}, m = 1, 2, 3, \ldots, \quad (1)$$

where $X_{m,t}$ denotes clean data; $noise_{m,t}$ denotes Gaussian white noise; and m, t denote trace number and time sampling point, respectively. The valid data in adjacent traces exhibit similar seismic characteristics in terms of interface and phase, indicating spatial correlation. Conversely, random noise, as a disordered time series, shows a lack of spatial correlation.

$$\begin{cases} X_{2m-1,t} \approx X_{2m,t} \\ noise_{2m-1,t} \neq noise_{2m,t} \end{cases}, \quad m = 1, 2, 3, \ldots. \quad (2)$$

Dividing the traces into two sub-gathers (G^A_{sub} and G^B_{sub}) based on the parity of the trace number and using them as the input and label of the network respectively can affect the learning rate of the network for valid data and random noise due to the correlation difference in space. In general,

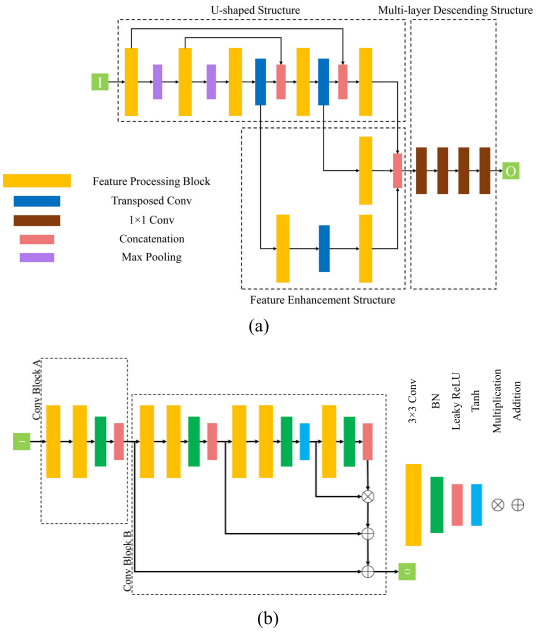

FIGURE 2. M-ResUNet framework. (a) Overall framework. (b) Feature processing module.

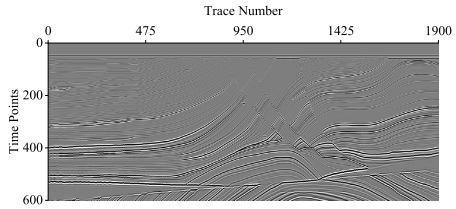

FIGURE 3. Synthetic original zone for training.

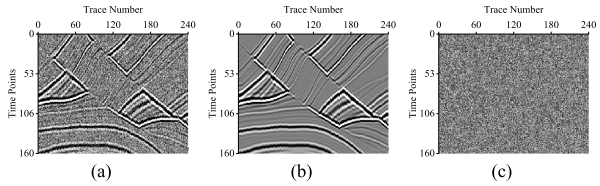

FIGURE 4. Synthetic example. (a) Noisy data. (b) Clean data. (c) Random noise.

the network can first finish the learning to valid data due to its higher spatial correlation. According to the theory of Gao et al. [26], if we can stop training at an appropriate epoch ($\varphi \in [E_{min}, E_{max}]$), the corresponding denoising model ($F_{Net}(\ :\ ;\varphi)$) can successfully map the valid data from the input (X_I) to those from the label (X_L). Simultaneously, this model can also map the random noise from the input ($noise_I$) to its expected value, which is 0, due to the influence of locally optimal solutions on parameter updating.

$$\begin{cases} F_{Net}\left(X_I;\varphi\right) = X_L \\ F_{Net}\left(noise_I;\varphi\right) = 0. \end{cases} \tag{3}$$

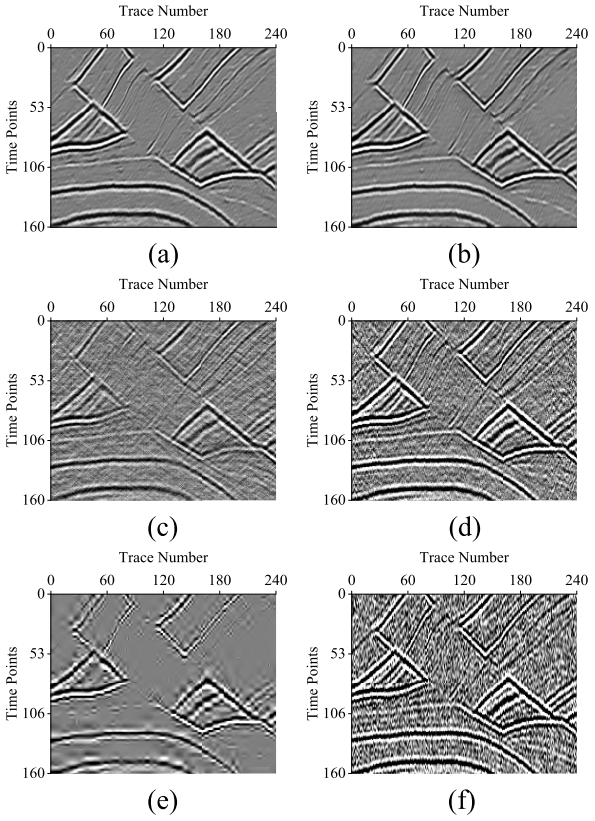

FIGURE 5. Denoising performances of synthetic example. (a)-(f) Denoising results: MRN-NEW, MRN-OLD, MSSA, FX, WT, and VMD.

This is equivalent to attenuating the random noise in the noisy data and reconstructing the valid data within it.

$$F_{Net}\left(Y_{m,t};\varphi\right) = F_{Net}\left(X_{m,t} + noise_{m,t};\varphi\right) \approx X_{m,t}. \tag{4}$$

B. SELECTION STRATEGY

In this approach, we initially identify smaller zones with a specified number, which determine the sources and quantity of training samples. Subsequently, each selected zone generates a pair of samples for training, as illustrated in Fig. 1(a). Therefore, the key to enhancing the quality of training data lies in the methodology employed to obtain these zones. Generally, the higher the diversity of the chosen zones, the more diverse the features they contain. Increased diversity in features signifies that the training data derived from these zones can significantly enhance the network's generalization capability.

Therefore, we can enhance the diversity of the zone set by diminishing the similarity between zones, thereby improving the quality of the training data. Specifically, each time a zone is selected, the similarity between this zone and each zone in the zone set will be analyzed. Only when the selected zone exhibits dissimilarity to any zone in the set, it will be utilized as a formal training data source and added to the zone set for participation in the next round of similarity comparison. Under this selection mechanism, complex structures in

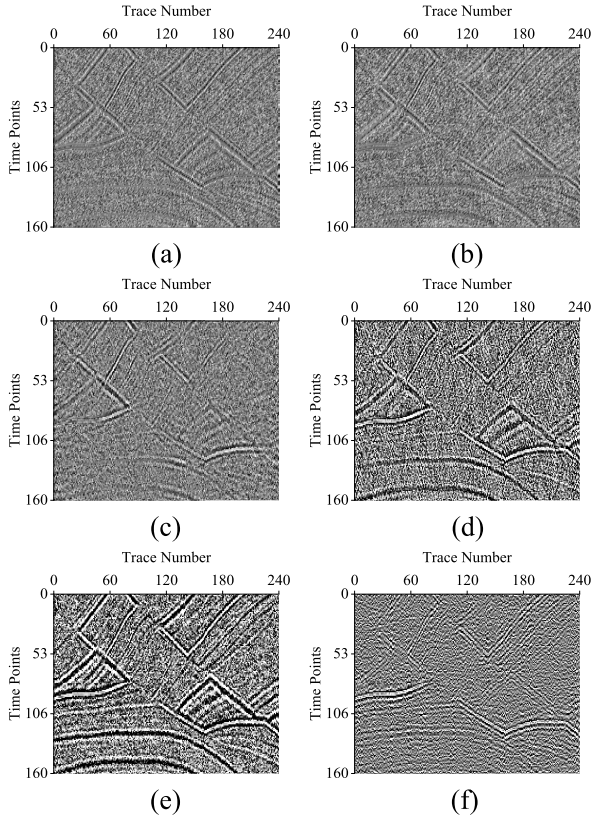

FIGURE 6. Denoising performances of synthetic example. (a)-(f) Removed noise: MRN-NEW, MRN-OLD, MSSA, FX, WT, and VMD.

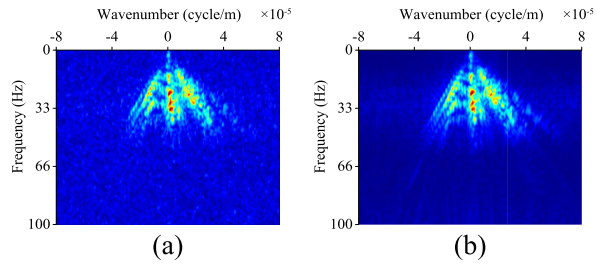

FIGURE 7. FK domain analysis. (a) Noisy data. (b) Clean data.

seismic data become easier to be selected due to their intricate geological characteristics. This leads to a higher proportion of data representing complex structures in the training dataset, thereby potentially enhancing the quality of the training data. Consequently, the network's ability to process complex structures and its generalization capacity can be improved. By employing this selection approach, we can acquire a sequence of high-quality training data sources characterized by high diversity.

C. SIMILARITY ANALYSIS AND LOSS FUNCTION

The similarity analysis can be performed using the Structure Similarity Index Measure (SSIM). SSIM is a perceptual model that quantifies the level of distortion in an image

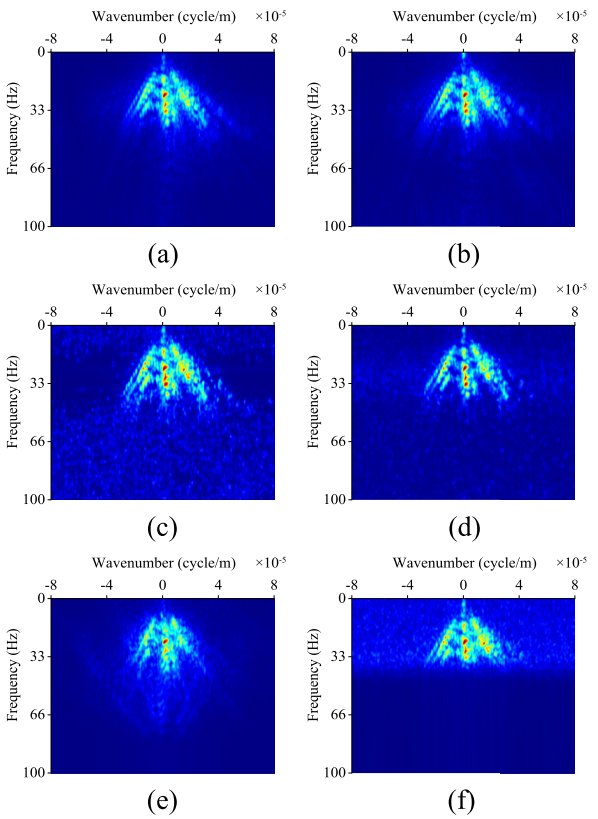

FIGURE 8. FK domain analysis for denoising results. (a) MRN-NEW. (b) MRN-OLD. (c) MSSA. (d) FX. (e) WT. (f) VMD.

and also measures the similarity between two images. This evaluation method can comprehensively assess images based on three aspects: luminance, contrast, and structure. We utilized SSIM and threshold a to quantify the level of similarity between the two zones. We supposed that if the SSIM value is less than or equal to the threshold a, it indicates a low similarity between the selected zone and the reference zone. In this article, the threshold a is set to 0.05.

The mean square error (MSE) is commonly employed to assess the network's training efficiency. The loss function in this article can be expressed as follows:

$$L(\theta) = \frac{1}{2M} \sum_{i=1}^{M} \left\| F_{Net}\left(B_i^I; \theta\right) - B_i^L \right\|_F^2 , \qquad (5)$$

where M represents the number of samples in the training set; $\|\cdot\|_F$ represents the Frobenius norm; B_i^I denotes the patches from the input; B_i^L denotes those from the label.

III. NETWORK ARCHITECTURE

In this article, we have adopted M-ResUNet [26] to exhibit the effectiveness of the proposed methodology, as shown in Fig. 2(a). M-ResUNet can break through the constraints of the U-shaped processing pathway in the conventional UNet network and conduct additional processing on certain feature maps to achieve superior training outcomes. The M-ResUNet network comprises three fundamental structures, namely

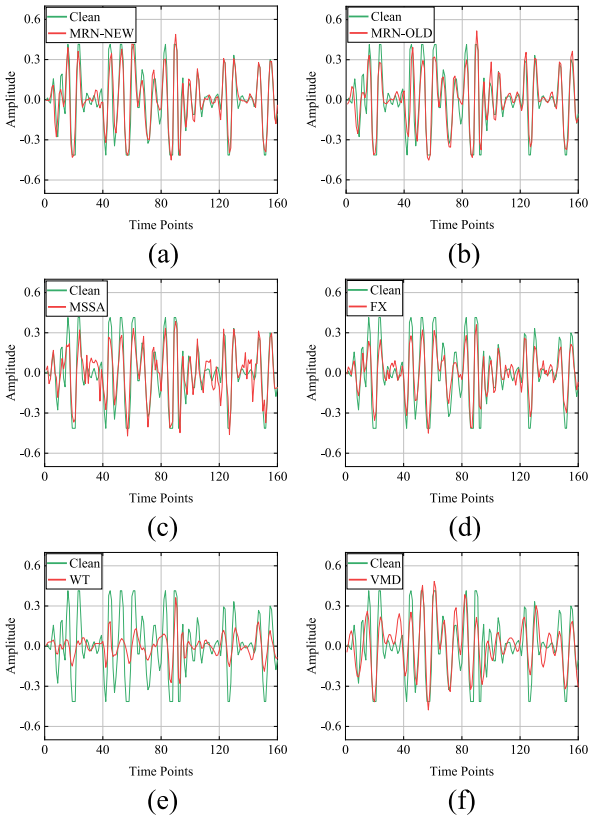

FIGURE 9. Amplitude comparisons on the 40th trace record. (a) MRN-NEW. (b) MRN-OLD. (c) MSSA. (d) FX. (e) WT. (f) VMD.

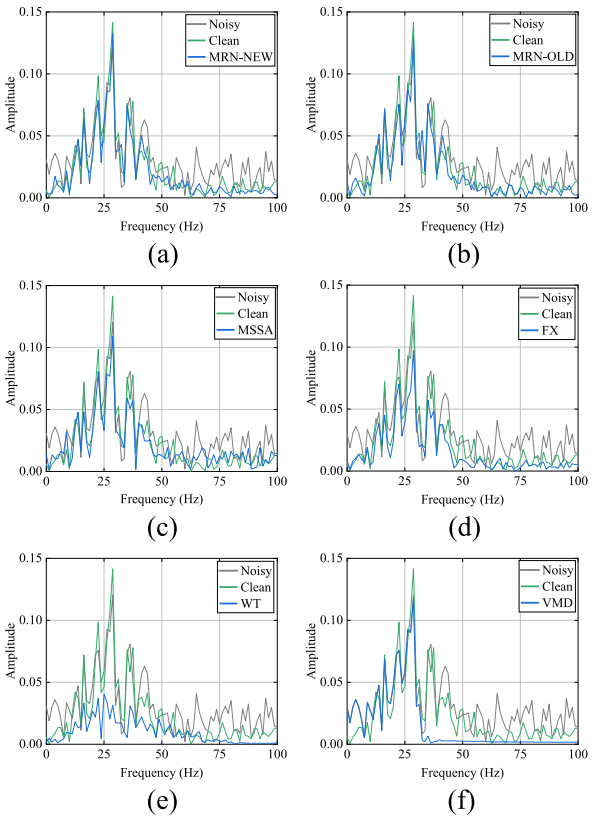

FIGURE 10. Spectrum comparisons on the 40th trace record. (a) MRN-NEW. (b) MRN-OLD. (c) MSSA. (d) FX. (e) WT. (f) VMD.

the U-shaped structure, feature enhancement structure, and multi-layer descending structure. The U-shaped structure serves to extract features at varying levels and provides an interface for subsequent processing of these features. The feature enhancement structure can not only perform additional processing on the features with a specified scale but also control the bias of the final output towards features of different scales by manipulating the ratio of the number of channels associated with these features. The multi-layer descending structure can not only reduce the extent of feature loss after convolution operations but also possess a larger parameter count and a broader parameter selection space, thereby expediting network learning.

In addition, there is a feature processing module consisting of two components, Conv Block A and Conv Block B, is adopted to further facilitate network learning, as shown in Fig. 2(b). Conv Block A expedites feature extraction across all data via consecutive double convolutions, while Conv Block B accelerates the update of the network parameter vector towards the specific local optimal solution with a denoising effect via a specific multiple residual structure.

IV. NUMERICAL RESULTS

All experiments were performed on a PC (Intel Core i5-12400F 2.50 GHz CPU, 16-GB memory, and an NVIDIA GeForce RTX 3060 GPU).

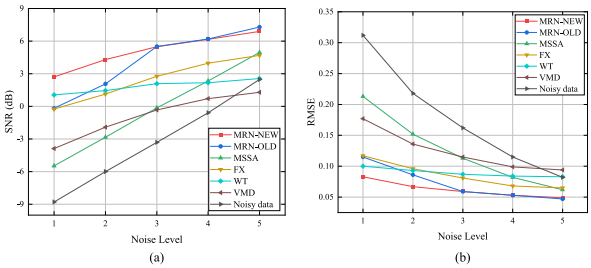

FIGURE 11. SNR and RMSE comparisons at different noise levels. (a) SNR comparison. (b) RMSE comparison.

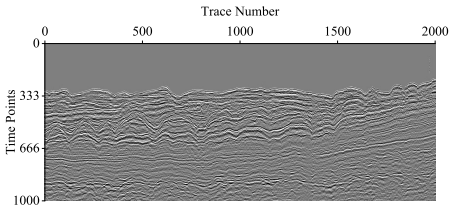

FIGURE 12. Field original zone for training.

A. DATA ANALYSIS

To quantitatively assess the denoising performance from different methods, the SNR and root mean squared error (RMSE) [27] were applied to evaluate the results. SNR and

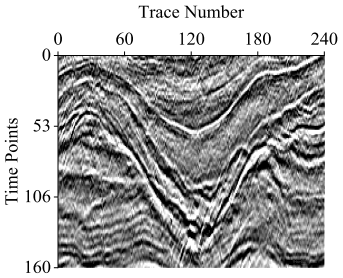

FIGURE 13. Field example.

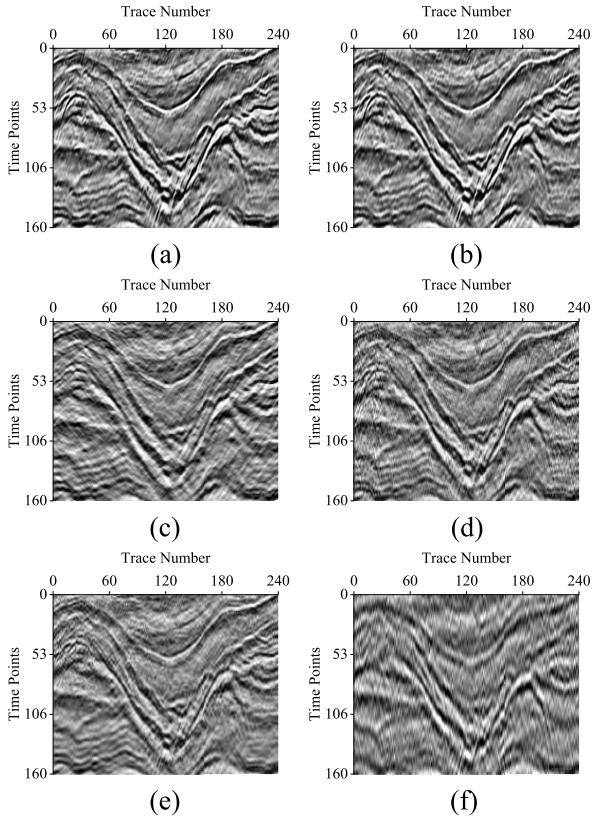

FIGURE 14. Denoising performances of field example. (a)-(f) Denoising results: MRN-NEW, MRN-OLD, MSSA, FX, WT, and VMD.

RMSE can be expressed as follows:

$$SNR = 10\log_{10}\left(\frac{\sum_{i=1}^{N}\sum_{j=1}^{M}\left(X_{i,j}\right)^2}{\sum_{i=1}^{N}\sum_{j=1}^{M}\left(F_{Net}\left(Y_{i,j}\right)-X_{i,j}\right)^2}\right), \quad (6)$$

$$RMSE = \sqrt{\frac{1}{NM}\sum_{i=1}^{N}\sum_{j=1}^{M}\left(F_{Net}\left(Y_{i,j}\right)-X_{i,j}\right)^2}, \quad (7)$$

where $F_{Net}\left(Y_{i,j}\right)$ and $X_{i,j}$ represent the denoising result and the clean data, respectively; M and N are the dimensions of the seismic data. In addition, it is impractical for conventional self-supervised denoising methods to evaluate the overall computational cost by individually processing small zones divided from the test zone. To provide a more accurate assessment of the cost, we have adopted the metric of computational cost per pixel (CCP), as follows:

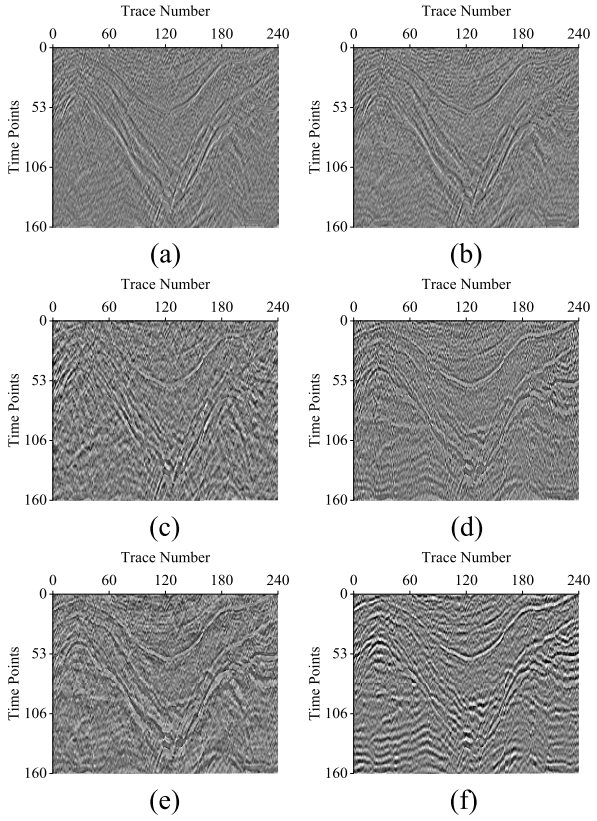

FIGURE 15. Denoising performances of field example. (a)-(f) Removed noise: MRN-NEW, MRN-OLD, MSSA, FX, WT, and VMD.

$$CCP = \frac{T_{prep} + T_{train}}{S}, \quad (8)$$

where T_{prep} denotes preparation time for training data construction; T_{train} denotes training time; S denotes the number of pixel in the training zone.

B. NETWORK TRAINING SETTINGS

In this article, we adopted the self-supervised method from Gao et al. [26] (MRN-OLD) for comparison, as shown in Fig. 1(b). The hyperparameters utilized by the proposed method (MRN-NEW) are the same as those of the MRN-OLD. Both methods utilized the Adam optimizer with an initial learning rate of 0.001. The patch size was set to 80×80, and the training set consisted of 384 samples. Both Trainings were conducted for 6 epochs. It is important to note that the training zone for the proposed method (MRN-NEW) encompasses the entire original zone. This means that it only needs to be trained once to process any zone within the original zone. However, the training zone of MRN-OLD is limited to its testing zone. Consequently, its processing for the entire original zone requires repeated and independent trainings.

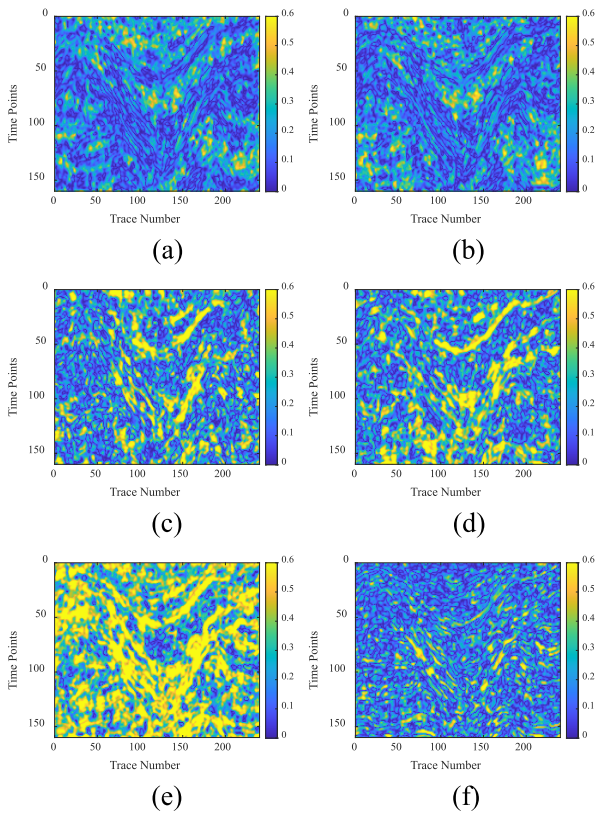

FIGURE 16. Denoising performances of field example. (a)-(f) Local similarity map: MRN-NEW, MRN-OLD, MSSA, FX, WT, and VMD.

C. EXPERIMENTS ON SYNTHETIC DATA

We utilized the post-stack data from the Marmousi2 model [28] to demonstrate the exceptional performance of our proposed method. Initially, we chose an original zone comprising 600 sampling points and 1900 traces for training the proposed method, as shown in Fig. 3. Subsequently, we selected a test zone consisting of 160 sampling points and 240 traces from the original zone to assess the denoising methods, which includes MRN-NEW, MRN-OLD, MSSA, FX, WT, and VMD. We added Gaussian white noise of 1dB to the test zone to create a synthetic example, which is shown in Fig. 4. The denoising results of MRN-NEW, MRN-OLD, MSSA, FX, WT, and VMD are shown in Fig. 5, along with their respective SNRs of 6.894 dB, 7.292 dB, 4.954 dB, 4.690 dB, 2.560 dB, and 1.287dB. The removed noise corresponding to each denoising result is displayed in Fig. 6. MRN-NEW and MRN-OLD exhibit similar and commendable performances in denoising and amplitude preservation, surpassing MSSA, FX, WT, and VMD. However, MRN-NEW demonstrates a lower computational cost compared to MRN-OLD, approximately one-twentieth of the cost from MRN-OLD, as shown in Table 1. This means that the proposed approach incurs substantially lower training costs than those associated with MRN-OLD.

Then, we conducted the FK analysis on the denoising results to better capture the distinctions between different methods. Fig. 7 displays the FK spectra of the synthetic example. Fig. 8(a)-(f) shows the FK spectra of MRN-NEW, MRN-OLD, MSSA, FX, WT, and VMD, respectively. MRN-NEW and MRN-OLD continue to exhibit comparable and commendable performances in noise reduction, surpassing traditional methods. In addition, we applied comparisons of amplitude and spectrum on the 40th trace record, as shown in Fig. 9 and Fig. 10. It is clear that MRN-NEW and MRN-OLD have similar performances in noise attenuation, which is better than traditional methods. Finally, we applied these methods to the synthetic example with five different levels of random noise and compared their SNRs and RMSEs in Fig. 11 and Table 2. It can be observed that MRN-NEW outperforms MRN-OLD at most noise levels and exhibits greater resilience to strong noise interference.

D. EXPERIMENTS ON FIELD DATA

To further prove the excellent performance of our proposed method, we utilized a set of post-stack data from U.S. East Coast seismic data. The original zone consisted of 1000 sampling points and 2000 traces, which were used to train the proposed method, as shown in Fig. 12. The test zone consists of 160 sampling points and 240 traces from the original zone, serving as a test zone to evaluate the denoising methods, as shown in Fig. 13. Table 3 shows the training details of MRN-NEW and MRN-OLD for field example. It's evident that the training cost per pixel for MRN-NEW is lower than that for MRN-OLD, despite MRN-NEW requiring more time to prepare the training data. The denoising results of MRN-NEW, MRN-OLD, MSSA, FX, WT, and VMD are presented in Fig. 14, while the corresponding removed noise can be observed in Fig. 15. It is worth noting that both MRN-NEW and MRN-OLD exhibit better performances than MSSA, FX, WT, and VMD. In addition, we made local similarity maps for these methods, as shown in Fig. 16. It is clear that self-supervised methods have less similarity than MSSA, FX, and WT, which means these self-supervised methods have better performance in amplitude preservation. Even if VMD shows a low local similarity, it has more obvious reflection events in its removed noise than self-supervised methods, which suggests VMD exhibits a worse performance in amplitude preservation.

V. CONCLUSION

Aiming to address the challenge of applying the self-supervised random noise suppression method to denoise seismic data with large volumes, we proposed a novel self-supervised denoising approach that can reduce calculation costs. The key feature of this method lies in its ability to identify more valuable data zones via correlation analysis, enabling the construction of a higher-quality training set. Consequently, the method only requires a single training process to enable it to attenuate noise in any zone within the original zone, which eliminates the need of individual processings for smaller zones. This results in a significant reduction in computational costs by minimizing the number

of individual processings. Experimental evaluations using synthetic and field data demonstrate the excellent performances of the proposed method in random noise attenuation and seismic signal reconstruction. However, we note that the denoising ability of our proposed method may degrade under extremely low signal-to-noise ratio (SNR) conditions. Moreover, the selection process of SSIM values can also contribute to a certain degree of time consumption. Despite these limitations, our proposed method has promising applications in complex random noise attenuation and seismic signal processing.

ACKNOWLEDGMENT

The authors would like to thank the reviewers and the journal's editors. Comments by the journal's editors and the associated reviewers are very helpful in improving the article.

REFERENCES

[1] S. M. Mousavi and G. C. Beroza, "Deep-learning seismology," *Science*, vol. 377, no. 6607, Aug. 2022, Art. no. eabm4470.

[2] G. Liu, X. Chen, J. Du, and K. Wu, "Random noise attenuation using f-x regularized nonstationary autoregression," *Geophysics*, vol. 77, no. 2, pp. V61–V69, Mar. 2012.

[3] D. Bonar and M. Sacchi, "Spectral decomposition with f-x-y preconditioning," *Geophys. Prospecting*, vol. 61, pp. 152–165, Feb. 2013.

[4] M. Bagheri, M. A. Riahi, and H. Hashemi, "Denoising and improving the quality of seismic data using combination of DBM filter and FX deconvolution," *Arabian J. Geosci.*, vol. 10, no. 19, pp. 1–8, Oct. 2017.

[5] K. Chen and M. D. Sacchi, "Robust f-x projection filtering for simultaneous random and erratic seismic noise attenuation," *Geophys. Prospecting*, vol. 65, no. 3, pp. 650–668, May 2017.

[6] H. Shan, J. Ma, and H. Yang, "Comparisons of wavelets, contourlets and curvelets in seismic denoising," *J. Appl. Geophys.*, vol. 69, no. 2, pp. 103–115, Oct. 2009.

[7] Z. Yu and D. Whitcombe, "Seismic noise attenuation using 2D complex wavelet transform," in *Proc. 70th EAGE Conf. Exhib. Incorporating SPE EUROPEC*, vol. 15, 2008, p. 40.

[8] N. Liu, Y. Yang, Z. Li, J. Gao, X. Jiang, and S. Pan, "Seismic signal denoising using time–frequency peak filtering based on empirical wavelet transform," *Acta Geophys.*, vol. 68, no. 2, pp. 425–434, Apr. 2020.

[9] S.-A. Ouadfeul and L. Aliouane, "Random seismic noise attenuation data using the discrete and the continuous wavelet transforms," *Arabian J. Geosci.*, vol. 7, no. 7, pp. 2531–2537, Jul. 2014.

[10] W. Liu, Y. Liu, S. Li, and Y. Chen, "A review of variational mode decomposition in seismic data analysis," *Surv. Geophys.*, vol. 44, pp. 323–355, Nov. 2022.

[11] F. Li, B. Zhang, S. Verma, and K. J. Marfurt, "Seismic signal denoising using thresholded variational mode decomposition," *Explor. Geophys.*, vol. 49, no. 4, pp. 450–461, Aug. 2018.

[12] T. P. Banjade, S. Yu, and J. Ma, "Earthquake accelerogram denoising by wavelet-based variational mode decomposition," *J. Seismol.*, vol. 23, no. 4, pp. 649–663, Jul. 2019.

[13] J. Feng, X. Liu, X. Li, W. Xu, and B. Liu, "Low-rank tensor minimization method for seismic denoising based on variational mode decomposition," *IEEE Geosci. Remote Sens. Lett.*, vol. 19, pp. 1–5, 2022.

[14] D. Zhang, Y. Chen, W. Huang, and S. Gan, "Multi-step damped multichannel singular spectrum analysis for simultaneous reconstruction and denoising of 3D seismic data," *J. Geophys. Eng.*, vol. 13, no. 5, pp. 704–721, 2016.

[15] Y. Zhang, H. Zhang, Y. Yang, N. Liu, and J. Gao, "Seismic random noise separation and attenuation based on MVMD and MSSA," *IEEE Trans. Geosci. Remote Sens.*, vol. 60, 2022, Art. no. 5908916.

[16] V. Oropeza and M. Sacchi, "Simultaneous seismic data denoising and reconstruction via multichannel singular spectrum analysis," *Geophysics*, vol. 76, no. 3, pp. V25–V32, May 2011.

[17] Y. Chen, W. Huang, D. Zhang, and W. Chen, "An open-source MATLAB code package for improved rank-reduction 3D seismic data denoising and reconstruction," *Comput. Geosci.*, vol. 95, pp. 59–66, Oct. 2016.

[18] J. Gao, Z. Li, M. Zhang, Y. Gao, and W. Gao, "Unsupervised seismic random noise suppression based on local similarity and replacement strategy," *IEEE Access*, vol. 11, pp. 48924–48934, 2023.

[19] C. Liang, H. Lin, and H. Ma, "Reinforcement learning-based denoising model for seismic random noise attenuation," *IEEE Trans. Geosci. Remote Sens.*, vol. 61, 2023, Art. no. 5908217.

[20] W. Zhu, S. M. Mousavi, and G. C. Beroza, "Seismic signal denoising and decomposition using deep neural networks," *IEEE Trans. Geosci. Remote Sens.*, vol. 57, no. 11, pp. 9476–9488, Nov. 2019.

[21] X. Dong, J. Lin, S. Lu, X. Huang, H. Wang, and Y. Li, "Seismic shot gather denoising by using a supervised-deep-learning method with weak dependence on real noise data: A solution to the lack of real noise data," *Surv. Geophys.*, vol. 43, no. 5, pp. 1363–1394, Oct. 2022.

[22] J. Li, X. Wu, and Z. Hu, "Deep learning for simultaneous seismic image super-resolution and denoising," *IEEE Trans. Geosci. Remote Sens.*, vol. 60, 2022, Art. no. 5901611.

[23] X. Dong, T. Zhong, and Y. Li, "A deep-learning-based denoising method for multiarea surface seismic data," *IEEE Geosci. Remote Sens. Lett.*, vol. 18, no. 5, pp. 925–929, May 2021.

[24] R. Tibi, P. Hammond, R. Brogan, C. J. Young, and K. Koper, "Deep learning denoising applied to regional distance seismic data in Utah," *Bull. Seismolog. Soc. Amer.*, vol. 111, no. 2, pp. 775–790, Apr. 2021.

[25] Q. Feng and Y. Li, "Denoising deep learning network based on singular spectrum analysis—DAS seismic data denoising with multichannel SVDDCNN," *IEEE Trans. Geosci. Remote Sens.*, vol. 60, 2022, Art. no. 5902911.

[26] J. Gao, Z. Li, and M. Zhang, "Seismic random noise attenuation based on M-ResUNet," *IEEE Trans. Geosci. Remote Sens.*, vol. 61, 2023, Art. no. 5913716.

[27] T. Zhong, M. Cheng, X. Dong, Y. Li, and N. Wu, "Seismic random noise suppression by using deep residual U-Net," *J. Petroleum Sci. Eng.*, vol. 209, Feb. 2022, Art. no. 109901.

[28] G. S. Martin, S. Larsen, and K. Marfurt, "Marmousi-2: An updated model for the investigation of AVO in structurally complex areas," in *Proc. SEG Int. Expo. Annu. Meeting*, Oct. 2002, pp. 1979–1982.

JIAN GAO received the B.S. degree in transportation from Inner Mongolia University, Huhhot, China, in 2020. He is currently pursuing the M.S. degree in geophysics with China University of Petroleum (East China).

His research interests include deep learning, swarm intelligence, and seismic data denoising and reconstruction.

ZHENCHUN LI received the B.S. and M.S. degrees in geophysics from China University of Petroleum (East China), Qingdao, China, in 1983 and 1991, respectively, and the Ph.D. degree in geophysics from Tongji University, Shanghai, China, in 2002.

He is currently the Director of SWPI, China University of Petroleum (East China). His research interest includes seismic wave forward propagation and imaging. He has won several honors, including the Outstanding Graduate Student Instructor; and the Second Prize of Science and Technology Progress in Shandong Province, China.

MIN ZHANG received the B.S. degree in computer science and the M.S. and Ph.D. degrees in geophysics from China University of Petroleum (East China), Qingdao, China, in 2005, 2007, and 2011, respectively.

She completed a joint Ph.D. training in geophysics with UT-Austin, Austin, USA. Since 2011, she has been a Senior Experimentalist with the School of Geoscience, China University of Petroleum (East China). Her research interests include illumination analysis and observation system optimization, seismic data denoising, seismic wave propagation and imaging, velocity inversion and modeling, and time-lapse seismic data processing. She has won the Excellent Instructor Award (many times) in the National Undergraduate Exploration Geophysics Competitions.

WANYUE GAO is currently pursuing the B.S. degree in logistics with Shandong Normal University.

Her research interests include supply chain management and deep learning.

YIXUAN GAO is currently pursuing the B.S. degree in biological science with Qufu Normal University.

Her research interests include swarm intelligence and deep learning.